

Supporting information

S@C Composites Constructed by Graded Pore-Making Strategy for Mg-S Battery with Outstanding Rate Performance

Peng Xue,^{a,#} Pengpeng Wang,^{b,#} Xuyan Qin,^b Zhikai Wang,^b Xi Jia^b and Wutao Wei^{b,}*

^{a.} School of Electrical and Information Engineering, Henan University of Engineering, Zhengzhou, 450007, Henan, PR China.

^{b.} Henan Key Laboratory of Functional Salt, Center for Advanced Materials Research, Zhongyuan University of Technology, Zhengzhou, 450007, Henan, PR China.

Corresponding Author: W. T. Wei (E-mail: 506952644@qq.com)

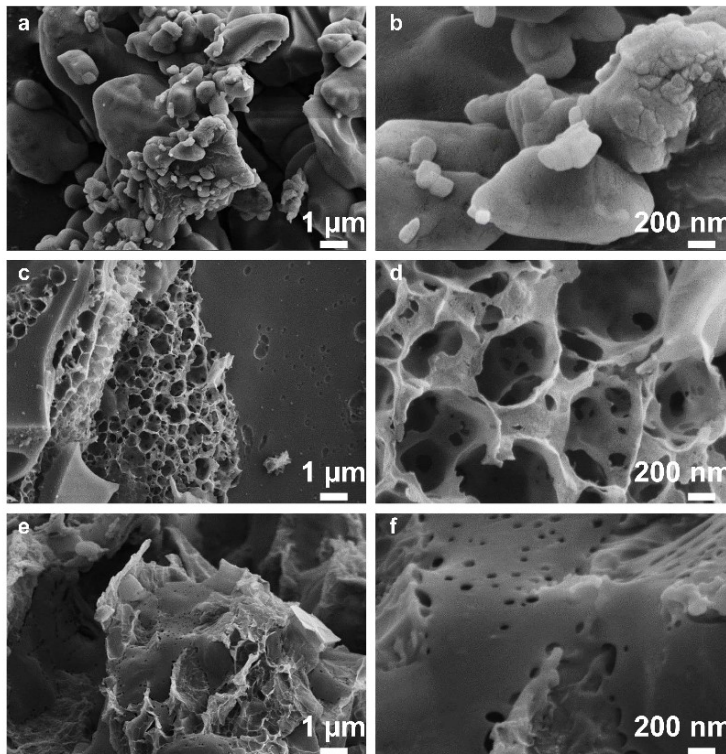


Fig. S1. (a), (b) High magnification and low magnification SEM patterns of C@NaCl material; (c), (d) High magnification and low magnification SEM patterns of porous carbon material; (e), (f) High magnification and low magnification SEM patterns of S@C material.

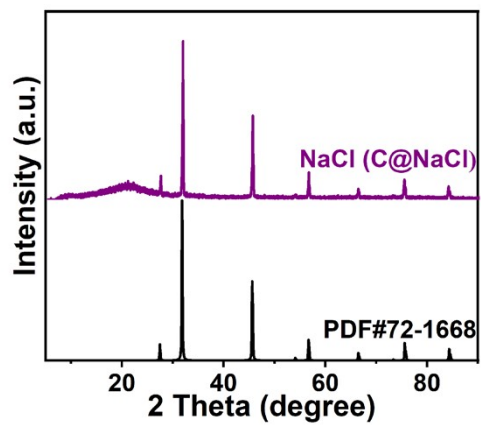


Fig. S2. C@NaCl XRD pattern.

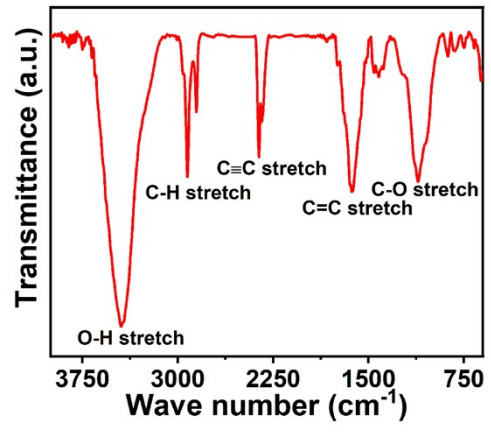


Fig. S3. Fourier infrared spectra (FTIR) of porous carbon materials.

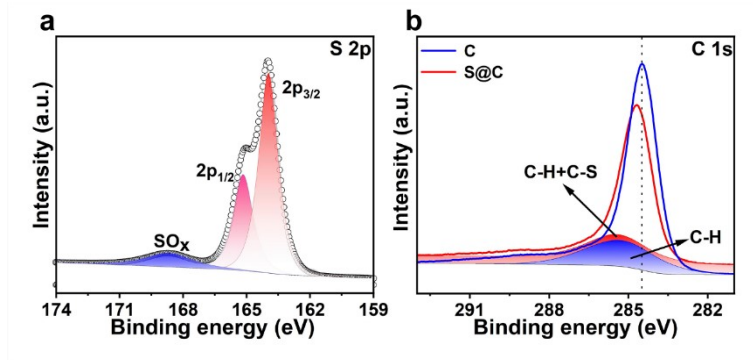


Fig. S4. (a) S@C material S 2p XPS spectrum; (b) XPS of porous carbon compared with S@C material C 1s.

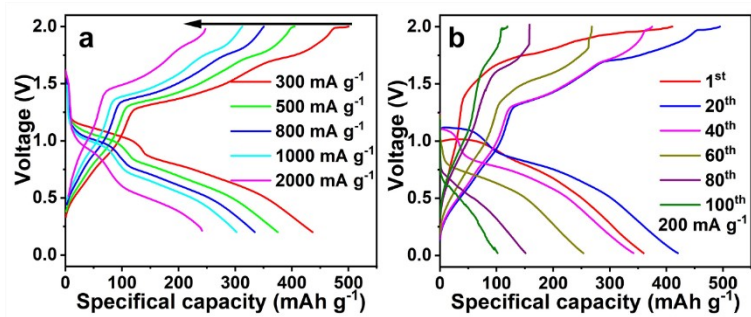


Fig. S5. (a) S@C charge discharge curves under different current densities; (b) S@C charge discharge curve at 200 mA g⁻¹ current density.

Table S1. $I_p-v^{1/2}$ slope and proton diffusion coefficient corresponded to different redox peaks.

Reaction peaks	$D_{Mg^{2+}}$
A	$2.35 \times 10^{-5} \text{ cm}^2 \text{ s}^{-1}$
B	$1.66 \times 10^{-5} \text{ cm}^2 \text{ s}^{-1}$
C	$2.11 \times 10^{-5} \text{ cm}^2 \text{ s}^{-1}$
D	$6.53 \times 10^{-5} \text{ cm}^2 \text{ s}^{-1}$

Fig. S6 shows the comparison of electrodes before and after the cycle, it can be seen that S@C material can still maintain the basic morphology after the cycle and is not broken, and the whole electrode remains intact after the cycle. Therefore, it can be inferred that S does not react with Cu, so that the electrode can remain intact. Fig. 6e and Fig. S7 are comparison diagrams of element distribution, it can also be seen that magnesium sulfide gradually forms on the surface of S@C material with the progress of charging and discharging.

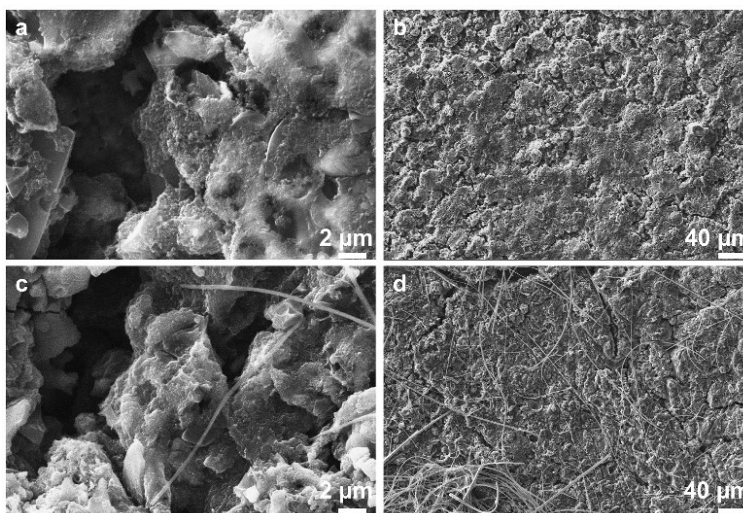


Fig. S6. (a), (b) S@C SEM image of the original electrode sheet of the material; (c), (d) SEM image of the electrode after 50 cycles.

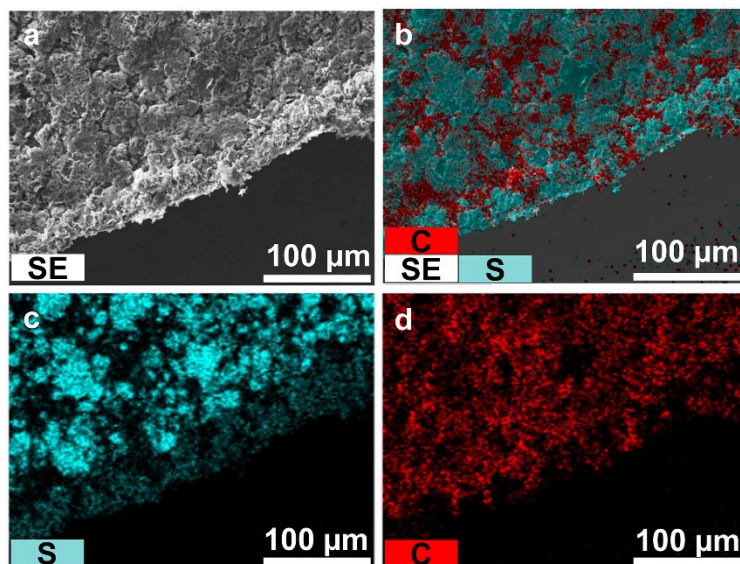


Fig. S7. Pre-cycle (a) SEM image of electrode sheet; (b-d) Distribution of C and S elements in the electrode sheet.

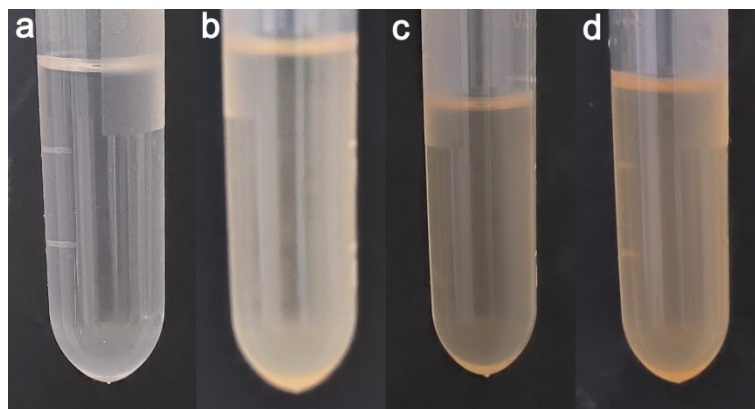


Fig. S8. (a) the $2\text{PhMgCl}/\text{THF}-\text{AlCl}_3$ electrolyte, (b) 0.2 M MgS in $2\text{PhMgCl}/\text{THF}-\text{AlCl}_3$ electrolyte, (c) 0.2 M MgS_4 in $2\text{PhMgCl}/\text{THF}-\text{AlCl}_3$ electrolyte and (d) 0.2 M MgS_8 in $2\text{PhMgCl}/\text{THF}-\text{AlCl}_3$ electrolyte.

As shown in Fig. S9, through the porous carbon material based on the battery performance test, it showed very poor performance in the multiplier and cycle, 50 mA g^{-1} , can only maintain about 3 mAh g^{-1} capacity, and the cycle is directly decreased after 20 turns. Therefore, S@C material is mainly sulfur element in providing capacity.

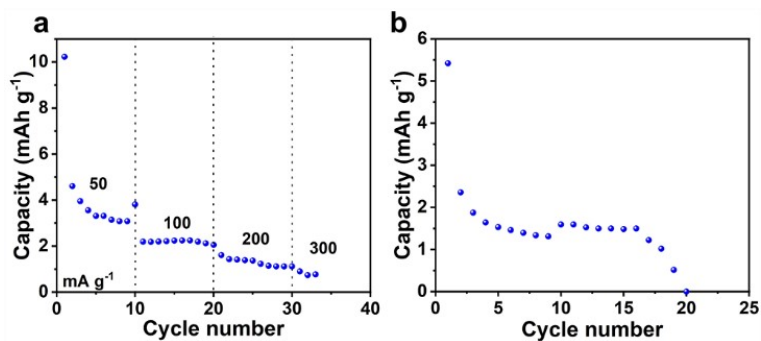


Fig. S9. Performance diagram based on porous carbon materials: (a) Magnification performance diagram; (b) Cycle performance diagram.